Highly Ordered Porous Zirconias from Surfactant-Controlled Syntheses: Zirconium Oxide−Sulfate and Zirconium Oxo Phosphate

Ulrike Ciesla,[†,§] Michael Fröba,[‡] Galen Stucky,[§] and Ferdi Schüth*[,†]

Institut für Anorganische Chemie, Johann Wolfgang Goethe-Universität, Frankfurt, Germany, Institut für Anorganische und Angewandte Chemie, Universität Hamburg, Hamburg, Germany, and Department of Chemistry, University of California−Santa Barbara, Santa Barbara, California

Received March 31, 1998. Revised Manuscript Received October 21, 1998

The syntheses and characterization of mesostructured hexagonally ordered surfactant composites using zirconium sulfate ions as inorganic precursor species are described. On the basis of the mesostructured zirconium sulfate surfactant composites, two porous MCM-41 analogues have been synthesized: zirconium oxide−sulfate and zirconium oxo phosphate. For the zirconium oxo phosphates, a special postsynthetic treatment has been developed. The pore arrangements and wall structures were characterized by XRD, nitrogen adsorption, EXAFS, and TEM. The porous zirconia based materials show hexagonal arrangements of uniformly sized pores and amorphous pore walls. Both zirconium oxide−sulfate and zirconium oxo phosphate show remarkable thermal stability up to 500 °C. Therefore, the surfactant has been completely removed from the structures by calcination. So far, this is the highest thermal stability compared to other porous transition metal oxides prepared via surfactant-controlled synthesis.

Introduction

In the search for catalytically interesting new mesoporous materials,[1,2] a number of synthetic strategies have been proposed to extend the composition of mesoporous materials to metal oxides other than silica.[3−5] So far, three major pathways have been developed, leading to mesostructured metal oxide surfactant composites. First, analogous to the MCM-41 synthesis and based on the charge interaction between anionic inorganic species (I^-) and cationic surfactant molecules (S^+), mesostructured metal oxide composites were prepared using tungsten,[6,7] antimony,[7] and molybdenum.[6] Moreover, the inversely charged system using inorganic polyoxo cations (I^+) and anionic surfactants (S^-) also leads to mesostructured composites. Iron-, lead-,[6] and titanium-based[8] surfactant composites were successfully prepared in the inversely charged system. Nonionic surfactants (S^0) have been used for the formation of mesostructured alumina.[9] In the case of silica, mesoporous monoliths[10] have been formed, which makes this synthesis very attractive. Additionally, Antonelli et al. developed a new so-called ligand-assisted synthesis.[11,12] The mechanism is based on the fact that bonds are formed between the inorganic species and the surfactant headgroups (S−I). Following this approach, mesostructured niobium[11] and tantalum oxides[12] were prepared by using surfactants with amine headgroups.

However, a major problem of these nonsiliceous oxide composites is thermal stability. The surfactant removal by calcination, as used for porous silicates, leads to structure collapse. It was assumed that incomplete condensation, in the case of tungsten oxide[13] and antimony oxide,[7] and redox reactions during the calcination process are responsible for the thermal instability. So far, four mesostructured oxides besides silica have been obtained as porous materials based on titania,[8] niobia,[11] tantalum oxide,[12] and zirconia[14,15] showing clearly a hexagonal pore arrangement analogous to

* To whom correspondence should be addressed. Permanent address: Max Planck Institut fur Kohlenforschung, Kaiser Wilhelm Platz 1, 45470 Mülheim. E-mail: schueth@mpi-muelheim.mpg.de.
† Johann Wolfgang Goethe-Universität.
‡ Universität Hamburg.
§ University of California.

(1) Corma, A.; Fornes, V.; Navarro, M. T.; Perez-Pariente, J. *J. Catal*. **1994**, *148*, 569.
(2) Sayari, A. *Chem. Mater.* **1996**, *8*, 1840.
(3) Kresge, C. T.; Leonowicz, M. E.; Roth, W. J.; Vartuli, J. C.; Beck, J. S. *Nature* **1992**, *359*, 710.
(4) Beck, J. S.; Vartuli, J. C.; Roth, W. J.; Leonowicz, M. E.; Kresge, C. T.; Schmitt, K. D.; Chu, C. T.-W.; Olson, D. H.; Sheppard, E. W.; McCullen, S. B.; Higgins, J. B.; Schlenker, J. L. *J. Am. Chem. Soc.* **1992**, *114*, 10834.
(5) Vartuli, J. C.; Kresge, C. T.; Roth, W. J.; McCullen, S. B.; Beck, J. S.; Schmitt, K. D.; Leonowicz, M. E.; Lutner, J. D.; Sheppard, E. W. *Proceedings of the 209th National Meeting*; American Chemical Society, Division of Petroleum Chemistry, Anaheim, 1995, 21.
(6) Ciesla, U.; Demuth, D.; Leon, R.; Petroff, P.; Stucky, G.; Unger, K.; Schüth, F. *J. Chem. Soc., Chem. Commun.* **1994**, 1387.
(7) Huo, Q.; Margolese, D.; Ciesla, U.; Feng, P.; Gier, T. E.; Sieger, P.; Leon, R.; Petroff, P.; Schüth, F.; Stucky, G. D. *Nature* **1994**, *368*, 317.
(8) (a) Antonelli, D. M.; Ying, J. Y. *Angew. Chem*. **1995**, *107*, 2202; *Angew. Chem., Int. Ed. Engl*. **1995**, *34*, 2014. (b) Fröba, M.; Muth, O.; Reller, A. *Solid State Ionics* **1997**, *101−103*, 249.
(9) Bagshaw, S. A.; Pinnavaia, T. J. *Angew. Chem*. **1996**, *108*, 1180; *Angew. Chem., Int. Ed. Engl.* **1996**, *35*, 1102.
(10) Attard, G. S.; Glyde, J. C.; Goeltner, C. G. *Nature* **1995**, *378*, 366.
(11) Antonelli, D. M.; Ying, J. Y. *Angew. Chem*. **1996**, *108*, 461; *Angew. Chem., Int. Ed. Engl.* **1996**, *35*, 426.
(12) Antonelli, D. M.; Ying, J. Y. *Chem. Mater*. **1996**, *8*, 874.
(13) Stein, A.; Fendorf, M.; Jarvie, T. P.; Mueller, K. T.; Bebesi, A. J.; Mallouk, T. E. *Chem. Mater.* **1995**, *8*, 874.

10.1021/cm980205v CCC: $18.00
Published on Web 01/05/1999

MCM-41 with BET surface areas (normalized to density) comparable to those obtained with silica.

Here, we focus on the synthesis of thermally stable mesostructured zirconia. Several synthesis routes, leading to mesostructured zirconia, have been described so far which are based on two main synthesis pathways, a templating[16] and a scaffolding[17,18] mechanism. The main difference is that the templated materials are distinguished by their ordered pore systems while products made via scaffolding show a disordered pore arrangement. Moreover, Sachtler and co-workers[19] prepared a spongelike mesoporous zirconia which shows a high degree of crystallinity in the pore walls. They found that the crystallization of the zirconia results in collapse of the mesoporous structure. We used zirconium sulfate as the zirconium source and alkyltrimethylammonium bromide as the surfactant. The surfactant composites are formed in a charged system anologous to the original MCM-41 synthesis (I^- and S^+) via a templating mechanism. According to the building mechanism known from MCM-41,[20,21] the inorganic precursor species are expected to form polydentate and polycharged molecular species, which coordinate electrostatically to the surfactant molecules. The charge, geometry, and association of the inorganic molecular species in solution can be adjusted by varying the pH, counterions, and temperature.[22] Following this approach, two new pathways have been developed to stabilize the porous phases of mesostructured transition metal oxides even after template removal by thermal treatment.

Experimental Section

Chemicals. Zirconium sulfate $Zr(SO_4)_2 \cdot 4H_2O$ (Alfa); zirconium propoxide $Zr(OC_3H_7)_4$, 70 wt % in 1-propanol (Aldrich); ammonium sulfate $(NH_4)_2SO_4$ (Aldrich); and phosphoric acid H_3PO_4, 85 wt % in H_2O, were used as received without further purification.

Surfactants. Cetyltrimethylammonium bromide was purchased from Aldrich and used as received. Octadecyltrimethylammonium bromide (Aldrich) was recrystallized from acetone/ethanol for purification. Surfactants showing an odd C-atom number or a C-atom number larger than C_{18} were prepared using the following synthesis:[23] 10 mmol of alkane bromide was dissolved in excess trimethylamine solution (33 wt % in ethanol). The crystalline precipitate was recrystallized from acetone/ethanol three times.

Synthesis. *Zirconium Oxide-Sulfate.* Hexadecyltrimethylammonium bromide (2.5 g, 6.87 mmol) was dissolved in a solution of water (115 g) and HCl (37 wt %, 24.4 g), and zirconium propoxide (12.8 mmol) was added. After the hydrolysis products had dissolved, $(NH_4)_2SO_4$ in water (23 g) was added and the mixture was stirred at room temperature for 1 h. The amount of $(NH_4)_2SO_4$ was dependent on the molar ratio SO_4 to Zr; calcinable samples were made by using SO_4/Zr molar ratios of 1.2−0.65. The initially clear solution was then heated at 100 °C for 2 days. The colorless precipitate was filtered, dried, and calcined at 500 °C for 5 h.

Zirconium Oxo Phosphate. The surfactant (6.87 mmol) was dissolved in water (85 g), and $Zr(SO_4)_2 \cdot 4H_2O$ (4.55 g, 0.0128 mol) dissolved in water (25 g) was added. (Surfactants with longer chain length than C_{18} were heated to 75 °C.) This led to a colorless precipitate. The mixture was stirred for 2 h at room temperature and then heated to 100 °C for 2 days in a closed polypropylene beaker. The precipitate was filtered and without drying added to a phosphoric acid solution (0.5 M) and stirred for 5 h. After filtration, the colorless product was calcined at 500 °C for 5 h.

The as-synthesized samples contain 40−50 wt % surfactant, as detected by thermogravimetric analysis between 20 and 600 °C.

Analysis. The structures of the samples were analyzed using a STOE Stadi P X-ray diffractometer in Debye−Scherrer geometry equipped with a position sensitive detector covering an angle range of 7.5° (2θ). Analyses were performed with Cu Kα radiation ($\lambda = 1.54056$ nm). A typical scan time for the range to 15° (2θ) was 20 min. Unless otherwise stated, samples do not have reflections at higher angles between 10° and 60° (2θ). Elemental composition of the samples were determined by X-ray fluorescence on pressed PVA pellets using a Philips PW 1400 and by using an inductively coupled plasma−atomic emission (ICP-AES) spectrometer. Sorptive analyses were carried out using a Micromeritics ASAP 2010 unit with nitrogen at 77.4 K. Samples were outgassed for 14 h at 250 °C. Pore size distributions were calculated following the density functional theory (DFT) with the routines supplied by Micromeritics. High-resolution transmission electron microscopy (TEM) images were obtained on a Philips EM 400 T transmission electron microscope operating at 100 kV. Samples were prepared by sonication in ethanol and suspension on carbon-coated copper grids. The X-ray absorption spectra were recorded at SSRL (Stanford Synchrotron Radiation Laboratory) with SPEAR (Stanford Positron Electron Accelerator) operating at an electron energy of 3 GeV and an injection current of 100 mA. BL 10-2 was used with a Si (220) double crystal monochromator. To reduce contributions from higher harmonics, the second crystal was detuned to 50% of the maximum intensity. All spectra were recorded in transmission at ambient temperature using a continuous scanning technique (QEXAFS).[24,25] The counting time per data point was between 0.1 and 0.2 s, and the distance between the data points was 2 eV for the EXAFS (extended X-ray absorption fine structure) spectra. The spectra were processed according to the common data reduction procedures using the program WinXAS.[26] The spectra were calibrated against the first inflection point of the Zr K-edge (17998 eV) of a Zr foil, which was measured simultaneously. The preedges were normalized for absorbance by fitting the spectra with a Victoreen function subtracting this as a background. Thereafter, the edge jump was normalized to a value of 1 for the absorption. Finally, the EXAFS oscillations were extracted by subtracting the atomic absorption μ_0. Least-squares refinements of the structure parameters were carried out by applying theoretical phase shifts and backscattering amplitudes which were calculated by using the program FEFF6.01.[27] It is well-known that the values for S_0^2, N, and σ are highly correlated. For this reason,

(14) Ciesla, U.; Schacht, S.; Stucky, G. D.; Unger, K. K.; Schüth, F. *Angew. Chem., Int. Ed. Engl.* **1996**, *35*, 541.
(15) Reddy, J. S.; Sayari, A. *Catal. Lett.* **1996**, *38*, 219.
(16) (a) Ualagappan, N.; Neeraj, B. V. N. Raju, C. N. R. Rao, *Chem. Commun*. **1996**, 2243. (b) Kim, A.; Bruinsma, P.; Chen, Y.; Wang, L.-Q.; Liu, J. *Chem. Commun*. **1997**, 161. (c) Jimenez-Jimenez, J.; Maireles-Torres, P.; Olivera-Pastor, P.; Rodriguez-Castellon, E.; Jimenez-Lopez, A.; Jones, D. J.; Roziere, J. *Adv. Mater.* **1998**, *10*, 812. (d) Wong, M. S.; Ying, J. Y. *Chem. Mater.* **1998**, *10*, 2067.
(17) (a) Hudson, M. J.; Knowles, J. A. *J. Chem. Soc., Chem. Commun*. **1995**, 1083. (b) Hudson, M. J.; Knowles, J. A. *J. Mater. Chem*. **1996**, *6*, 89.
(18) (a) Pacheco, G.; Zhao, E.; Garcia, A.; Sklyarov, A.; Fripiat, J. J. *Chem. Commun*. **1997**, 491. (b) Pacheco, G.; Zhao, E.; Garcia, A.; Sklyarov, A.; Fripiat, J. J. *J. Mater. Chem*. **1998**, *8*, 219.
(19) Huang, Y.-Y.; McCarthy, T. J.; Sachtler, W. M. H. *Appl. Catal.* **1996**, *148*, 135.
(20) Monnier, A.; Schüth, F.; Huo, Q.; Kumar, D.; Margolese, D.; Maxwell, R. S.; Stucky, G. D.; Krishnamurty, M.; Petroff, P.; Firouzi, A.; Janicke, M.; Chmelka, B. F. *Science* **1993**, *261*, 1299.
(21) Chen, C.-Y.; Burkett, S. L.; Li, H.-X.; Davis, M. E. *Microporous Mater.* **1993**, *2*, 27.
(22) Livage, J.; Henry, M.; Sachez, C. *Prog. Solid State Chem*. **1988**, *18*, 259.
(23) Jaeger, D. A.; Russell, S. G.; Suinozaki, H. *J. Org. Chem*. **1994**, *59*, 7544.
(24) Frahm, R. *Nucl. Instrum. Methods* **1988**, *A270*, 578.
(25) Frahm, R.; Wong, J. *Jpn. J. Appl. Phys.* **1993**, *32*, 188.
(26) Ressler, T. *J. Synchrotron Radiat.* **1998**, *5*, 118.
(27) Rehr, J. J.; Mustre de Leon, J.; Zabinsky, S. I.; Albers, R. C. *J. Am. Chem. Soc.* **1991**, *113*, 5135.

Table 1. Refined Structure Parameters[a] of the Zr K-EXAFS Analyses of Zirconium Oxide−Sulfates and Zirconium Oxo Phosphates

E_0 (eV)	S_0^2	N	R (Å)	$\Delta\sigma^2$ (Å^2)	N	R (Å)	$\Delta\sigma^2$ (Å^2)
		Zr Oxide−Sulfate, as Made					
		(Zr−O) 5.01	2.11	0.0046	(Zr−O) 4.1	2.28	0.0046
−3.06		(Zr−S) 2.39	3.43	0.0025	(Zr−Zr) 0.83	3.56	0.003
		Zr Oxide−Sulfate, Calcined					
		(Zr−O) 5.36	2.11	0.005	(Zr−O) 2.91	2.27	0.005
−0.96		(Zr−S) 1.1	3.32	0.0025	(Zr−Zr) 0.84	3.45	0.003
		m-ZrO_2					
	0.69	(Zr−O) [4]	2.1	0.0032	(Zr−O) [3]	2.24	0.0031
		Zr Oxo Phosphate, as Made					
		(Zr−O) 3.87	2.1	0.05	(Zr−O) 3.37	2.27	0.05
−3.59		(Zr−S) 1.95	3.43	0.0035	(Zr−Zr) 1.09	3.54	0.0041
		Zr Oxo Phosphate, after $H_3PO_4^-$ Treatment					
−1.52		(Zr−O) 5.13	2.09	0.0042	(Zr−O) 1.76	2.27	0.0041
		Zr Oxo Phosphate, Calcined					
		(Zr−O) 5.12	2.07	0.0034	(Zr−O) 1.36	2.25	0.0034
−0.42		(Zr−P) 0.87	3.22	0.0025	(Zr−Zr) 1.32	3.38	0.0035
		$Zr(SO_4)_2 \cdot 4H_2O$					
	0.93	(Zr−O) [8]	2.18	0.0041			

[a] N = coordination number, R = bond length, $\Delta\sigma^2$ = Debye−Waller factor, E_0 = photoabsorption energy threshold, S_0^2 = amplitude reduction factor. Fixed values are given in square brackets.

a simultaneous refinement of all three parameters will most likely lead to incorrect results. As we were predominantly interested in the determination of the coordination numbers, we first had to find reliable values for S_0^2 and σ. Therefore, we have started our calculations with two reference compounds, one for each group. Monoclinic zirconia was used for the zirconium oxide−sulfates and $Zr(SO_4)_2 \cdot 4H_2O$ for the zirconium oxo phosphates. The coordination numbers were fixed to their known values and S_0^2, R, and σ were refined (Table 1). The extracted distances (R) were in good agreement with theoretical values.[28,29] The determination reduction factors (S_0^2) (m-ZrO_2, 0.69; $Zr(SO_4)_2 \cdot 4H_2O$, 0.93) were kept constant and used for every compound in the respective group. In addition, the Debye−Waller factors of the first two Zr−O shells were constrained to be equal during their refinement.

Results and Discussion

Mesostructured Zirconium Sulfate Surfactant Composite. Zirconium exhibits a very pronounced polyoxo ion chemistry in aqueous solution.[22] Depending on the counterion, a large number of possibilities are conceivable for preparing mesostructured surfactant composits. Here, we focus on the coordination interaction between positively charged surfactant molecules and zirconium sulfate as the inorganic precursor species, leading to mesostructured MCM-41 analogues.

Sulfate groups show a quite high complexing ability (α = 32%) and are thus able to replace coordinated

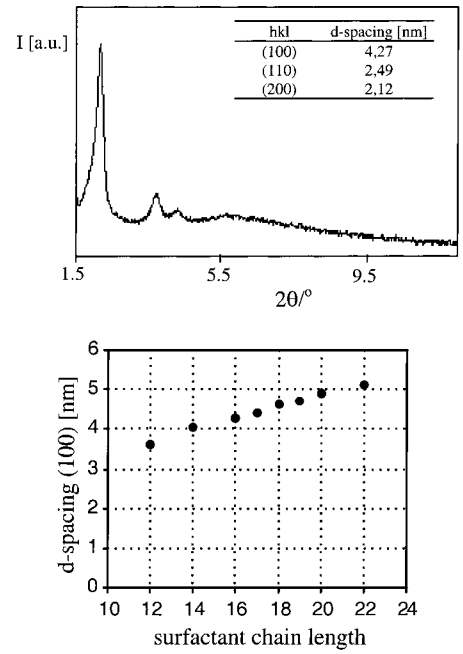

Figure 1. (a) XRD pattern of mesostructured zirconium sulfate−surfactant composite using hexadecyltrimethylammonium bromide as surfactant. (b) Dependence of the (100) reflection d-value on the surfactant chain length. The numbers correspond to the numbers of C-atoms of the chain.

water molecules. Moreover, sulfate molecules behave like network formers, bridging different chains together. Crystalline zirconium sulfates form structures of $Zr(OH)_2(SO_4)H_2O$[30] or $Zr(OH)_2(SO_4)$.[31] Therefore, a general polyoxo ion can be formulated assuming the structures of zirconium sulfate in aqueous solution: $[Zr(OH)_2(SO_4)_x(OH_2)_y]_n^{-n(2x-2)}$. Via the sulfate groups, charge interactions with the surfactant headgroups can occur. The XRD pattern of the zirconium sulfate surfactant composite shows only reflections in the low-angle region and very large lattice parameters, which is typical for mesostructured materials (Figure 1a). The reflections can be indexed assuming a hexagonal unit cell. The d spacings depend on the surfactant chain length, as it is expected for surfactant-controlled syntheses: the longer the surfactant chain length, the larger the d spacings of the (100) reflections (Figure 1b). Sayari et al.[32] observed an even−odd effect, obtaining lamellar or hexagonal mesophases depending on the number of carbon atoms in the dialkyldimethylammonium surfactants. In the studies reported here, no such even−odd effect of the surfactant is observed (Figure 1b). Moreover, using benzyldimethylstearylammonium chloride $[C_{18}H_{37}N(CH_3)_2(CH_2)C_6H_5Cl]$ as surfactant, it is possible to prepare the composite possessing the cubic structure.[33] The obtained XRD pattern can be indexed analogous to the MCM-48 material in the spacegroup $Ia3d$.

As observed before, for many other transition metal oxides the calcination of the surfactant composites

(28) Li, P.; Chen, I.-W.; Penner-Hahn, J. E. *Phys. Rev. B* **1993**, *48*, 109063.
(29) Singer, J.; Cromer, D. T. *Acta Crystallogr.* **1959**, *12*, 719.
(30) Hansson, M. *Acta Chem. Scand.* **1973**, *27*, 2614.
(31) El Brahimi, M.; Durand, J.; Cot, L. *Eur. J. Solid. State Inorg. Chem.* **1988**, *25*, 185.
(32) Sayari, A.; Karra, V. R.; Reddy, J. S. *Proceedings of the 209th National Meeting*; American Chemical Society, Division of Petroleum Chemistry, 1995, 228.
(33) Schüth, F.; Ciesla, U.; Schacht, S.; Thieme, M.; Huo, Q.; Stucky, G. *Mater. Res. Bull.* in print.

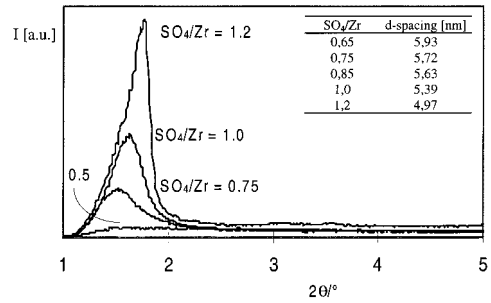

Figure 2. XRD pattern of as made zirconium oxide−sulfate sythesized by using sulfate-to-zirconium ratios of $SO_4/Zr = 0.5$ to $SO_4/Zr = 1.2$.

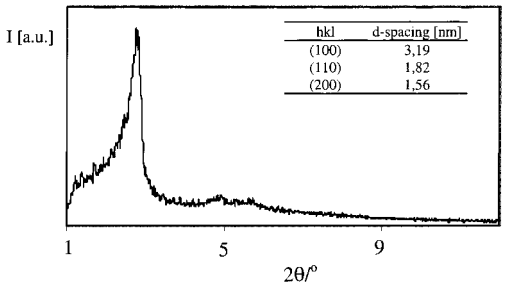

Figure 3. XRD pattern of calcined zirconium oxide−sulfate using a sulfate-to-zirconium ratio of $SO_4/Zr = 1.2$ and hexadecyltrimethylammonium bromide as surfactant.

results in a (partial) structure collapse. The same holds for composites synthesized from alkytrimethylammonium bromide and zirconium sulfate, if the materials are not further treated.[14] The mesostructure collapses and dense zirconium oxide is formed. Assuming that the thermal instability is due to the high quantity of sulfate groups, which decompose during thermal treatment, two methods to stabilize the ordered pore structure have been developed: (1) reduction of the sulfate amount by varying the original synthetic parameters leads to porous zirconia, so-called "zirconium oxide−sulfate"; (2) using a special postsynthetic treatment with phosphoric acid yields thermally stable materials, designated as "zirconium oxo phosphates".

Zirconium Oxide−Sulfates.[34] For the preparation of the thermally stable zirconium oxide−sulfates, the original synthesis procedure was changed: instead of using zirconium sulfate $Zr(SO_4)_2$ as the zirconium precursor, zirconium propoxide was used in combination with an appropriate amount of ammonium sulfate to form the zirconium sulfate species in aqueous solution.

The influence of sulfate content on the quality of the formed mesostructured composites can be observed by looking at the (100) reflection in the XRD pattern, shown in Figure 2. In the following six zirconium oxide−sulfate samples with SO_4/Zr molar ratios of 0.5−1.2 were investigated. From the analysis of the XRD pattern of the surfactant composites, three conclusions can be drawn: the reduction of the sulfate amount results in (1) a decrease of the intensity of the (100) reflection, (2) a shift of the (100) reflections to larger *d* spacings, and (3) a decrease in the intensity of the higher order reflections with reduction in sulfate content. Therefore, a compromise has to be made between forming a well-ordered mesostructure and obtaining a calcinable material by reduction of sulfate content.

To remove the surfactant, the zirconium oxide−sulfate mesostructures were calcined at 500 °C. After calcination the materials show highly intense (100) reflections and higher order (110) and (200) reflections (Figure 3). The large shift (≈1.0 nm) of the (100) reflections to smaller *d* spacings in comparison to the uncalcined samples due to a shrinkage of the pores during calcination is remarkable. The shrinkage becomes greater with increasing sulfate concentrations. Nitrogen adsorption analyses indicate that the zirconium oxide−sulfates are microporous, showing exclusively isotherms of the type I[35] (Figure 4a). The pore size analysis using the density functional theory (DFT)[36,37] gives narrow pore size distributions and shows a decrease in pore sizes with increasing sulfate

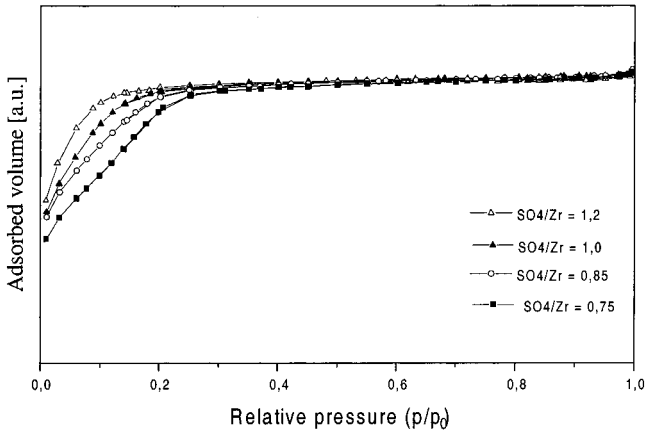

Figure 4. (a) Nitrogen adsorption−desorption isotherms of calcined zirconium oxide−sulfates synthesized with sulfate-to-zirconium ratios from 0.75 to 1.2. Hexadecyltrimethylammonium bromide was used as surfactant. For better comparison, the isotherms are normalized. (b) Pore size distribution of zirconium oxide−sulfate for different sulfate-to-zirconium ratios:[38] $SO_4/Zr = 0.65$ (---), $SO_4/Zr = 0.85$ (—), $SO_4/Zr = 1.2$: (— — —).

(34) "Zirconium oxide−sulfate" is not a term recommended by the IUPAC. However, we wanted to avoid terms such as "sulfated zirconia" or "zirconium oxo sulfate" which are terms used in the literature for other materials with specific chemical and physical properties.

(35) Gregg, S. J.; Sing, K. S. W. *Adsorption, Surface Area and Porosity*, 2nd ed.; Academic Press: London 1995.

(36) Ravikovitch, P. I.; Domhnaill, S. C. O.; Neimark, A. V.; Schüth, F.; Unger, K. *Langmuir* **1995**, *11*, 4765.

(37) On the basis of the density functional theory and a program, DFT, designed by Micromeritics and included in the software package ASAP 2010.

Figure 5. Transmission electron micrograph of zirconium oxide−sulfate showing the hexagonally ordered pores and additionally lamellar structures similar to a fingerprint.

amount: 2.5 nm for $SO_4/Zr = 0.65$ and 1.9 nm for $SO_4/Zr = 1.2$ (Figure 4b).[38] Moreover, the wall thicknesses were calculated by determining the differences in lattice parameters[39] and the pore sizes obtained from nitrogen adsorption analysis. The wall thicknesses clearly depend on the sulfate content and range from 1.9 nm ($SO_4/Zr = 1.2$) to 3.5 nm ($SO_4/Zr = 0.65$). However, one should bear in mind that so far no reliable algorithms exist for the analysis of pore size distributions from adsorption data in the micropore and lower mesopore range. The values given are thus only estimates.[38]

The pore structure is elucidated by transmission electron microscopy. The micrograph shows two different structural features: one part shows the hexagonally ordered pore structure which is expected from the X-ray analysis (Figure 5). Additionally, less ordered regions as well as structures that look like a fingerprint are visible. Similar structures have also been detected in MCM-41 materials by Alfredsson et al.[40] and were identified by Feng et al.[41] as disclination defects which are well-known in liquid crystal systems.

(38) The obtained absolute values of the pore sizes are probably incorrect: The parameters used in the DFT analysis (interaction of nitrogen on carbon and slit pores as pore geometry) are not realistic. However, trends can be correctly observed and values can be compared with each other.

(39) $a = b = 2d(100)/\sqrt{3}$ for hexagonal lattices with no order in the *c*-direction.

(40) Alfredsson, V.; Keung, M.; Monnier, A.; Stucky, G. D.; Unger, K. K.; Schüth, F. *J. Chem. Soc., Chem. Commun.* **1994**, 921.

(41) Feng, J.; Huo, Q.; Petroff, P. M.; Stucky, G. D. *Appl. Phys. Lett.* **1997**, *71*, 620.

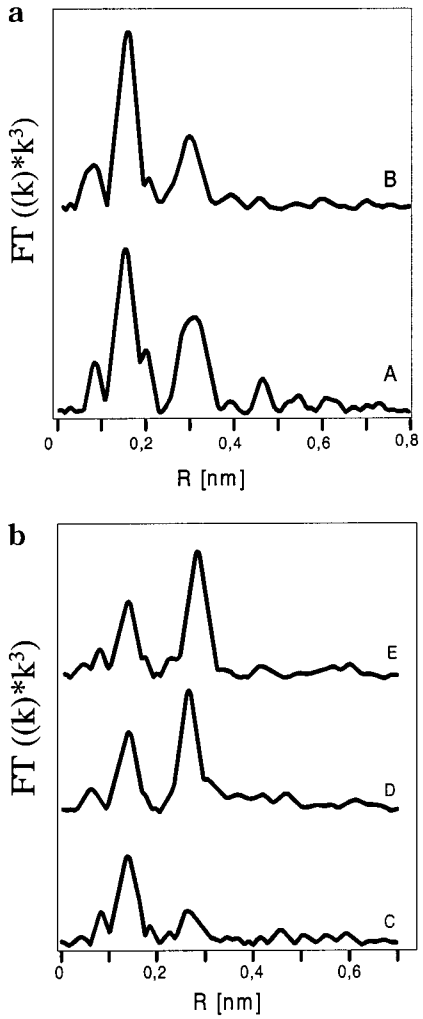

Figure 6. (a) Fourier-transformed Zr−K EXAFS spectra of zirconium oxide−sulfate: (A) as-made and (B) calcined. (b) Fourier transformed Zr−K EXAFS spectra of sulfated zirconia: (E) monoclinic, (D) tetragonal, and (C) amorphous.

Using X-ray absorption spectroscopy (XAFS), the local ordering in the walls has been investigated in detail. The Fourier transforms (FTs) of the EXAFS (extended X-ray absorption fine structure) spectra (Figure 6a) for the as-made sample and for the calcined sample show two broad peaks that can be divided into four different coordination spheres. The first two are formed by oxygen atoms with two different bond lengths. The third corresponds to a Zr−S shell. The remaining sphere within the second broad peak of the FT is due to zirconium as the backscattering atom. Depending on the stage of treatment, as-synthesized or calcined at 500 °C, the coordination numbers of the two Zr−O shells move in different directions. In the case of the first coordination sphere, an increase can be measured, whereas a reduction occurs for the second Zr−O shell (Table 1). Taking the experimental error into account, a small reduction in the sum of the Zr−O coordination numbers can be detected. The calcination increases the structural ordering within the inorganic network. Simultaneously, one can see a reduction in the coordination number of the higher shells as well as a shortening of the corresponding bond length, which could be an indication of a transition from loose gel to a slightly condensed and more ordered phase. Since the chemical composition of the zirconium oxide−sulfates is identical to that of

Table 2. Summarized Properties of Zirconium Oxide−Sulfate Synthesized with SO_4 to Zr Molar Ratios of 0.65−1.2

SO_4/Zr	$d_{(100)}$ (nm) as made	$d_{(100)}$ (nm) calcined	$d_{(100)}$ (nm) difference[a]	lattice parameter *a* (nm)	pore size (nm)	pore volume (mL/g)	S content of calcined sample (wt %)
0.65	5.93	5.15	0.78	5.95	2.5	0.07	5.8
0.75	5.72	4.80	0.92	5.54	2.4	0.125	7.2
0.85	5.63	4.20	1.43	4.85	2.2	0.125	6.9
1.0	5.39	3.57	1.82	4.12	2.0	0.126	5.3
1.2	5.06	3.07	1.99	3.70	1.9	0.113	8.5

[a] As made − calcined.

sulfated zirconias, which are important as acidic catalysts,[42] the FTs were compared with each other. It is obvious that the zirconium oxide−sulfates are most similar to the amorphous sulfated zirconia sample when comparing the FTs with those obtained for sulfated zirconia showing either the amorphous, monoclinic, or tetragonal phase (Figure 6b). Therefore, this result explains the relatively poor acidic properties and low conversions of zirconium oxide−sulfates in the butane isomerization reaction,[43] since for only the crystalline phases of sulfated zirconias can high catalytic activity be observed. This result is in good agreement with the data by Sachtler and co-workers[19] using sulfated mesoporous zirconia, who found catalytic activity only in the presence of crystalline t-ZrO_2.

In Table 2, the properties of zirconium oxide−sulfate with different SO_4/Zr ratios are summarized: zirconium oxide−sulfates are microporous materials with a pore arrangement similar to that of MCM-41.

Zirconium Oxo Phosphate. Since the high content of thermally unstable sulfate groups in the mesostructured $Zr(SO_4)_2$−surfactant composite is responsible for structure collapse during the calcination, a postsynthetic treatment of the as-made material has been developed: the mesostructured $Zr(SO_4)_2$−surfactant composite is treated with 0.5 M phosphoric acid solution. During the treatment the probably uncondensed ZrOH groups can be connected. Moreover, it is probable that coordinated water molecules and sulfate groups are replaced by phosphate groups, because phosphate groups (α = 50%) show an even stronger complexing ability than sulfate.[22] The XRD pattern after the phosphoric acid treatment is similar to the as-made composite material, except for a small 0.1 nm shift of the reflections to larger *d* spacings. After calcination at 500 °C, the materials show highly intense (100) reflections and weak (110) and (200) reflections. Figure 7 shows the dependence of the XRD patterns of the calcined materials on the surfactant chain length C_{16} to C_{22}. As observed for MCM-41, the increase of the surfactant chain length results in a shift of the reflections to larger *d* spacings. During calcination a strong shrinkage of the pores occurs which can be seen in the shift of the (100) reflections to smaller *d* spacings of more than 1 nm. The calcined zirconium oxo phosphates contain 10 wt % phosphorus and less than 0.2 wt % sulfur. The composition of the zirconium oxo phosphates is therefore: $4ZrO_2 \cdot P_2O_5(+SO_4)$. Figure 8a shows the nitrogen adsorption isotherms. Zirconium oxo phosphate prepared with C_{16} surfactant shows only the existence of micropores. Variation of the surfactant chain length leads to a shift of the step in the isotherm: the use of longer

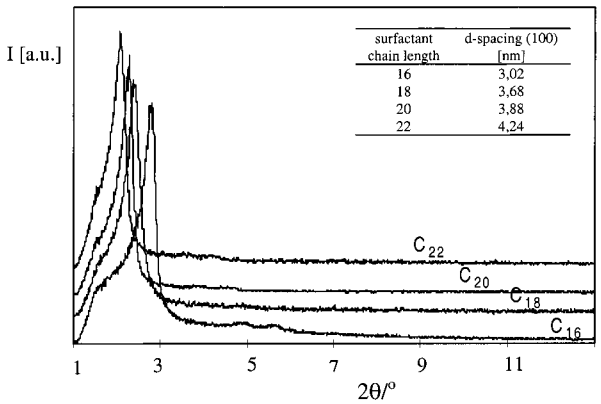

Figure 7. XRD patterns of calcined zirconium oxo phosphate using surfactant chain lengths of C_{16}, C_{18}, C_{20}, and C_{22}.

surfactant chain length shifts the step to higher p/p_0 values. This is an indication of the existence of larger pores, which is confirmed by the pore size analysis using the DFT method (Figure 8b). The pore size distribution is narrow, comparable to that in silica analogues. Depending on the surfactant chain length, materials could be obtained with pore sizes ranging from 1.8 nm (C_{16}) to 2.2 nm (C_{18}) to 2.5 nm (C_{20}) to 2.9 nm (C_{22}).[38] The results from the nitrogen adsorption measurements are in good agreement with the data obtained from the X-ray analysis. The pore volumes of the zirconium oxo phosphates are in the range of 0.17−0.26 cm^3/g (Table 3). Calculations of the BET surface areas of these materials are not reliable because the calculation is based on multilayer adsorption of the adsorbate on the adsorbent surface,[35] which does not take place in micropores and pores whose diameter is in the range between micro- and mesopores.

The wall thicknesses of the zirconium oxo phosphates can be determined by the combination of the results from X-ray diffraction and nitrogen adsorption. The wall thickness is determined to be 1.8−2.0 nm and is independent of the surfactant chain length. Therefore, the walls seem to be about twice as thick as the MCM-41 silicate walls. This result is confirmed by the transmission electron micrograph, which is shown in Figure 9a. However, an exact determination of wall thicknesses and pore diameters cannot be made without corresponding computer simulations of these micrographs. This is due to the focus problem, which is well-known in electron microscopy. Davis et al.[44] investigated the images of different focus adjustments in the case of MCM-41 and showed the dependence of the apparent wall thickness as well as of the pore diameter by varying the focus. The TEM micrograph of the zirconium oxo

(42) Corma, A. *Chem. Rev.* **1995**, *95*, 559.
(43) Suharto, T.; Ciesla, U.; Schüth, F. Unpublished result.
(44) Chen, C. Y.; Xiao, S.-Q.; Davis, M. E. *Microporous Mater.* **1995**, *4*, 1.

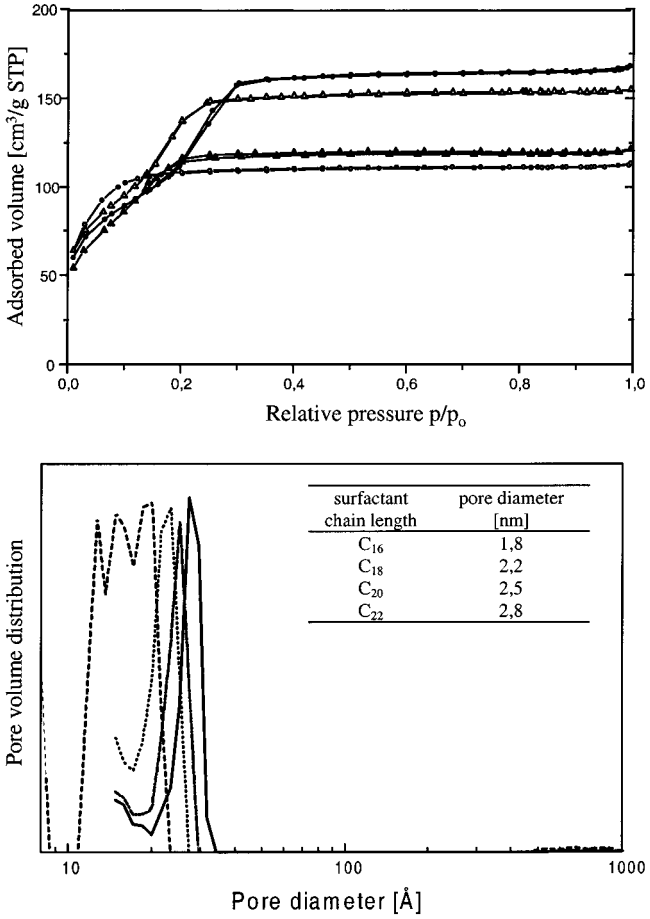

Figure 8. (a) Nitrogen adsorption−desorption isotherms of calcined zirconium oxo phosphates synthesized with different surfactant chain length: ○, $C_{16}H_{33}N(CH_3)_3Br$; ▲, $C_{18}H_{37}N(CH_3)_3Br$; △, $C_{20}H_{41}N(CH_3)_3Br$; ●, $C_{22}H_{45}N(CH_3)_3Br$. (b) Pore size distribution of zirconium oxo phosphates synthesized with different surfactant chain length.[38]

Table 3. Properties of Zirconium Oxo Phosphate Prepared with Surfactant Chain Length of C_{16}−C_{22}

surfactant chain length	d spacing (nm) phosphate treated	d spacing (nm) calcined	BET surface area (m^2/g)	pore volume (mL/g)
C_{16}	4.33	3.02	373	0.17
C_{18}	4.80	3.68	455	0.18
C_{20}	5.14	3.88	540	0.24
C_{22}	5.54	4.24	412	0.26

phosphate synthesized with C_{20} surfactant shows a very large, nicely ordered structure array with a hexagonal pore arrangement. Moreover, Figure 9b shows an enlarged part of this picture. Apart from the pore structure, the focus problem becomes obvious: two "kinds" of pores can be detected in this TEM micrograph: pores which are white surrounded by black walls and, in the same picture, black pores with white walls. Depending on the focus the apparent pores sizes and wall thicknesses change.

EXAFS studies of the zirconium oxo phosphates showed results similar to those obtained for the zirconium oxide−sulfates (Figure 10). As a function of the treatment—as-synthesized, post-treated with phosphoric acid, or calcined—the samples show an increase/decrease of the coordination numbers of the two Zr−O shells (Table 1). The treatment of the sample can be followed by changes in the structural order: While the coordination number of the Zr−Zr shell remains relatively constant, the coordination number of corresponding Zr−S and Zr−P shells will be reduced by postsynthesis treatment and calcination. Without any thermal but after phosphoric acid treatment, the FT of the zirconium oxo phosphate exhibits only the two Zr−O shells, an effect which is caused by a higher degree of disorder in the walls introduced by phosphoric acid. On the other hand, all bond lengths show a decrease after thermal treatment, which indicates the strong impact of calcination on the structural order of the material.

Thermal Stability. Zirconium oxide−sulfate and zirconium oxo phosphate are calcinable at 500 °C while a high surface area and an ordered pore structure are retained. These temperatures are sufficiently high to remove the surfactant completely from the structure. So far, these materials show the highest thermal stability compared to other mesoporous transition metal oxides. Only at temperatures between 600 and 750 °C does the pore structures collapse and denser oxides are formed. In both zirconium oxide−sulfate and zirconium oxo phosphate, the tetragonal zirconium oxide phase is formed, which is typical for sulfate- and phosphate-stabilized zirconias.[45,46,47]

It is well-known for sulfated[48] and phosphated zirconia[47] that crystallization occurs in the temperature range of 600−750 °C. Sulfate and phosphate anions are responsible for a crystallization delay, shifting the crystallization temperature to higher values. Pure untreated zirconias crystallize, depending on the preparation method, at temperatures below 400 °C.[49] Therefore, the anion contents of 5−8 wt % sulfate in the zirconium oxide−sulfates or 10 wt % phosphate in the zirconium oxo phosphates are responsible for the stabilization of the amorphous phase at temperatures up to 600 °C. Upon reaching the crystallization temperature, the collapse of the pore structure occurs. Therefore, the stabilization of the new porous zirconia compounds is based on the crystallization delay stabilizing the amorphous phase and thus the mesostructure.

Taking this into consideration, the thermal instability of the mesoporous transition metal oxides is understandable, because in general transition metal oxides crystallize at temperatures below 500 °C, which should at least be the calcination temperature to remove the surfactant. The collapse of the pore structure during calcination is also probably the reason that, so far, only amorphous mesostructures exist. Titania gels, for example, crystallize at temperatures of 300−400 °C.[50] At higher temperatures, anatase is formed. Therefore, the highest calcination temperature which can be used while the mesostructure is retained is 350 °C.[8] However, stabilization of the amorphous titania phase up to 550 °C is possible using the postsynthetic phosphate treatment developed for zirconia, leading to thermally stable titanium oxo phosphates.[51]

(45) Norman, C. J.; Goulding, P. A.; McAlpine, I. *Catal. Today* **1994**, *20*, 313.
(46) Afanasiev, P.; Geantet, C.; Breysse, M. *J. Mater. Chem.* **1994**, *4*, 1653.
(47) Parida, K. M.; Pattanyak, P. K. *J. Colloid Interface Sci.* **1996**, *182*, 381.
(48) Ward, D. A.; Ko, E. I. *J. Catal.* **1994**, *150*, 18.
(49) Hino, M.; Kobatashi, S.; Arata, K. *J. Am. Chem. Soc.* **1979**, *101*, 6439.
(50) Raggai, J.; Lofti, W. *Colloids Surf.* **1991**, *61*, 97.

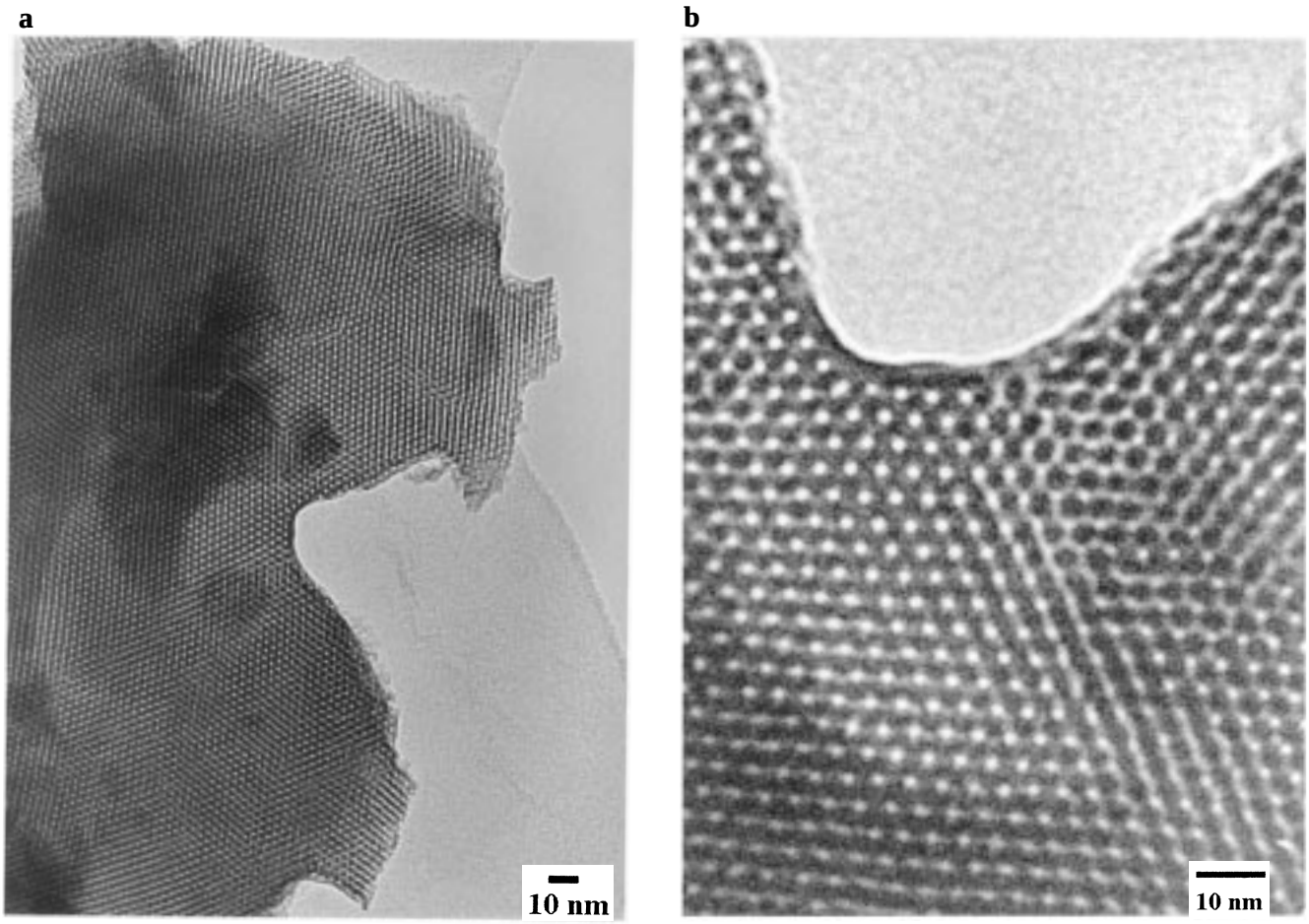

Figure 9. (a) Transmission electron micrograph of zirconium oxo phosphate synthesized with icosyltrimethylammonium bromide $C_{20}H_{41}N(CH_3)_3Br$ as surfactant. (b) Enlarged part of the transmission electron micrograph of zirconium oxo phosphate synthesized with icosyltrimethylammonium bromide $C_{20}H_{41}N(CH_3)_3Br$ as surfactant.

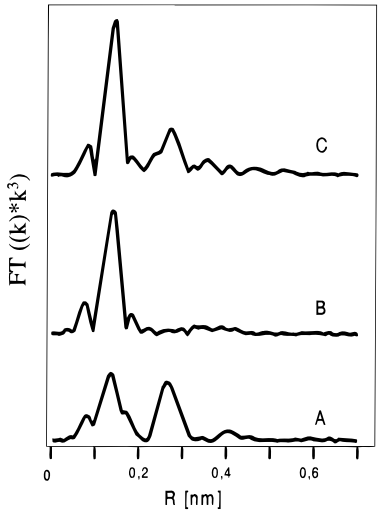

Figure 10. Fourier-transformed Zr−K EXAFS spectra of zirconium oxo phosphate. (A) as made zirconium sulfate surfactant composite, (B) as made composite after phosphate treatment, and (C) calcined zirconium oxo phosphate.

Conclusion

Hexagonally ordered mesostructured surfactant composites based on zirconia have been synthesized by using cationic surfactants and zirconium sulfate as the inorganic precursor species. The thermal stability of the zirconia-based materials was improved by the existence of a small amount of sulfate or phosphate groups in the walls. Therefore, complete surfactant removal by calcination at 500 °C was possible, resulting in the formation of new highly porous structures: zirconium oxide−sulfate and zirconium oxo phosphate. The sulfate and phosphate groups are responsible for inhibiting crystallization and stabilizing the amorphous zirconia phase. Porous zirconia-based materials possess a hexagonal pore arrangement showing a narrow pore size distribution. By combination of XRD, nitrogen adsorption, EXAFS, and TEM it was shown that both zirconium oxide−sulfate and zirconium oxo phosphate possess structures analogous to MCM-41.

Acknowledgment. This work was supported by the Deutsche Forschungsgemeinschaft (SCHU 744/8-1), by the NATO (CRG 950169), and by the National Science Foundation under DMR-9634396. We like to thank Dr. Y. Uchida and Prof. Dr. R. Schloegl from the Fritz Haber-Institut, Berlin, Germany, for recording the TEM micrographs. The synchrotron experiments were carried out at SSRL, supported by the U.S. Department of Energy, Division of Chemical Science. M.F. thanks SSRL for allocating beamtime and Dr. J. Wong (LLNL) for help during the XAFS measurements.

CM980205V

(51) Thieme, M.; Schüth, F. *Microporous Mesoporous Mater.* In press.